Journal of Food Science and Technology (Iran)

Homepage:www.fsct.modares.ir

Scientific Research

# Modeling the Release of Rosemary Essential Oil from Zein-Pectin Multilayer Films: Effect of Layer Sequence and Encapsulation Method on Film Properties

Ahmad Rajaei [1*], Narges Nazari [2], Hossein Mirzaee Moghaddam[3*]

1-Associate Professor, School of Agricultural Engineering, Shahrood University of Technology, Shahrood, Iran

2-Master of Food Science and Engineering, School of Agricultural Engineering, Shahrood University of Technology, Shahrood, Iran

3-Assistant Professor, School of Agricultural Engineering, Shahrood University of Technology, Shahrood, Iran

**ARTICLE INFO**

**Article History:**

Received: 2025/05/17
Accepted: 2025/07/01

**Keywords:**

Active packaging,

Biodegradable films,

Nanoemulsion,

Pickering emulsion.

DOI: **10.48311/fsct.2025.84050.0**

*Corresponding Author E-Mail:

ahmadrajaei@gmail.com

Hosseinsg@Yahoo.com

**ABSTRACT**

Biodegradable active films incorporating essential oils (EOs) often face challenges such as poor EO retention and inadequate physicomechanical properties. This study investigated the influence of layer sequence and encapsulation method (nanoemulsion vs. Pickering emulsion) on the release kinetics, physicomechanical properties of zein-pectin multilayer films containing rosemary essential oil (REO). Zein-basil seed gum (BSG) complex nanoparticles (D50 = 306.9 nm, ζ = -15.1 mV) were synthesized to stabilize Pickering emulsions (D50 = 1046.5 nm), while Tween 80-stabilized nanoemulsions (D50 = 90.1 nm) served as a control. Rheological analysis revealed shear-thinning behavior in Pickering emulsions, contrasting with the near-Newtonian flow of nanoemulsions. Multilayer films with pectin as the bottom layer exhibited smoother surfaces, higher tensile strength (TS), and lower water vapor permeability (WVP) compared to zein-bottomed films, attributed to pectin's superior homogeneity. Pickering emulsion incorporation enhanced TS and reduced WVP due to particle-matrix interactions, while nanoemulsions acted as plasticizers, increasing flexibility. REO release followed pseudo-Fickian diffusion, with pectin-bottomed films and nanoemulsions facilitating faster release, whereas zein layers and Pickering emulsions prolonged retention. These findings demonstrate that strategic layer arrangement and emulsion selection can improve EO delivery and film performance, offering tailored solutions for active food packaging.

## 1- Introduction

Biodegradable films offer substantial advantages over traditional plastic films, primarily in their environmental impact. They decompose naturally, reducing the accumulation of non-biodegradable waste in landfills and oceans, and thereby mitigating pollution and harm to wildlife. Preparing edible films from bio-macromolecules like pectin and zein offers notable advantages due to their natural, renewable origins and beneficial properties. However, biodegradable and edible films often have lower physic-mechanical properties compared to traditional plastics, limiting their use in certain applications (Alias, Wan, & Sarbon, 2022; Gupta, Biswas, & Roy, 2022). Active packaging is an innovative approach to food packaging that goes beyond the traditional passive role of containment and protection. It interacts with the food or the environment to extend shelf life, enhance safety, and maintain quality (Yang et al., 2024). Essential oils, complex mixtures of volatile compounds derived from plants, have attracted considerable attention from researchers for use in active packaging due to their multiple biological activities (Mutlu-Ingok, Devecioglu, Dikmetas, Karbancioglu-Guler, & Capanoglu, 2020). Meanwhile, rosemary essential oil (REO) has been widely studied for its beneficial biological properties. Various studies have used REO as an active agent in active packaging (Akhter, Masoodi, & Wani, 2024; Shahrampour & Razavi, 2023). Biodegradable active films containing essential oils face issues such as poor retention of essential oil compounds and insufficient mechanical properties (Zhang, Ismail, Cheng, Jin, Qian, Arabi, & Guo, 2021). In recent years, several promising methods such as multilayer films, nanoemulsions, and Pickering emulsions have been proposed to improve the release of essential oils from films (Zhang, Jiang, Rhim, Cao, & Jiang, 2022). Classical emulsions are stabilized by surfactants, which are molecules with hydrophilic (water-attracting) and hydrophobic (water-repelling) ends that reduce surface tension and prevent the coalescence of the dispersed phase droplets within the continuous phase. In contrast, Pickering emulsions are stabilized by solid particles especially nanoparticles that adsorb at the liquid-liquid interface, creating a mechanical barrier that prevents droplet coalescence. These particles can be inorganic or organic and their size and surface properties are crucial for the stability and type of emulsion formed (Hosseini, Rajaei, Tabatabaei, Mohsenifar, & Jahanbin, 2019; Sharkawy, Barreiro, & Rodrigues, 2020). The results of various studies have shown that Pickering emulsions can act as carriers of essential oils and protect these compounds from external factors, as well as cause the gradual release of essential oils (Pandita, Souza, Gonçalves, Jasińska, Jamróz, & Roy, 2024). Various compounds, including proteins and polysaccharides, have been employed to produce solid particles for stabilizing Pickering emulsions (Sharkawy & Rodrigues, 2024; Yang, Gupta, Du, Aghbashlo, Show, Pan, & Rajaei, 2023). *Ocimum basilicum* L., commonly known as basil and belonging to the Lamiaceae family, is a plant of significant economic and medicinal value. Basil seed gum (BSG) exhibits numerous biological activities, such as antimicrobial, prebiotic, antioxidant, antidiabetic, and cholesterol-lowering effects. Recent studies have successfully produced stabilizing particles from a combination of BSG and zein, which have been used to stabilize various Pickering emulsions (Chen, Wang, Rao, Lei, Zhao, & Ming, 2023; Wu, Zhang, Jiang, Hou, Xin, Zhang, & Zhou, 2022). Solid particles used in Pickering emulsions can interact with the matrix of active films, enhancing their mechanical and barrier properties. For instance, incorporating marjoram essential oil into a pectin film in the form of a Pickering emulsion has been shown to improve the release of the essential oil

as well as the physical and mechanical properties of the films (Almasi, Azizi, & Amjadi, 2020). Additional research has focused on achieving a sustained release of essential oils from films (Alinaqi, Khezri, & Rezaeinia, 2021; Papadaki, Lappa, Manikas, Carbone, Natsia, Kachrimanidou, & Kopsahelis, 2024). However, the direction of essential oil release from the film has not been thoroughly investigated. In food packaging, the inner layer contacts the food, while the outer layer is exposed to the environment. It is crucial to minimize the diffusion of essential oil towards the outer layer and maximize diffusion towards the inner layer. Multilayer films with different structures offer a potential solution to direct the diffusion of essential oils towards the inner layer. This study hypothesizes that the sequence of forming multilayer films influences the direction of essential oil diffusion. Additionally, the synergistic effects of layer formation and the method of essential oil encapsulation may impact the release of essential oil and the physical and mechanical properties of the films. Therefore, the objective of this study was to develop three-layer films with zein and pectin as the outer layers and encapsulated essential oil (nanoemulsion stabilized with Tween 80 and Pickering emulsion stabilized with BSG-zein particles) as a middle layer. Next, the microstructure, physico-mechanical properties of multi-layered films, as well as the kinetics of essential oil release were investigated.

## 2. Materials and Methods

### 2.1. Materials

Pectin (Degree of methyl esterification of 53%), Tween 80, zein, ethanol, and glycerol were procured from Sigma-Aldrich (Germany). The REO was purchased from Barij Essence Co. (Iran). The main components of the REO were described by the producer as α-pinene (23.6%), cineole (11.1%), camphor (7.7%), borneol (6.5%), limonene (4.3%), *P*-cymene (1.5%), β-pinene (1.1%). Basil seeds were procured from Shahroud local market.

### 2.2. Pickering emulsion and nanoemulsion containing REO

#### 2.2.1. Preparation of emulsions

Basil seed gum (BSG) was extracted following the method outlined by Jouki et al (Jouki, Yazdi, Mortazavi, & Koocheki,2013). Subsequently, for the production of the REO Pickering emulsion, a complex of zein-BSG particles was prepared. To prepare these particles, a 1% (w/v) solution of zein in 70% ethanol and a 1% (w/v) solution of BSG in distilled water were first prepared. The zein solution and BSG solution were then mixed in a 1:1 ratio and homogenized using an ultrasonic probe homogenizer (Sigmsonic, Iran) at an intensity of 750 W for 5 minutes (5 seconds on and 5 seconds off). Following homogenization, the ethanol solvent was evaporated using a rotary vacuum evaporator (Heidolph, Germany). The REO Pickering emulsion was then prepared by adding REO to the zein-BSG particles at a 1:4 ratio. This mixture was homogenized for 2 minutes using an Ultrathorax device (IKA, Germany) at 10,000 rpm. The primary emulsion was further homogenized using an ultrasonic homogenizer for 5 minutes (5 seconds on and 5 seconds off) at an intensity of 750 W. For the preparation of the nanoemulsion of REO, a combination of essential oil (1% w/v), Tween 80 (30% w/w of REO), and distilled water was mixed for 5 minutes using an Ultrathorax device at 10,000 rpm. This mixture was then homogenized with an ultrasonic probe homogenizer (Sigmsonic, Iran) at an intensity of 750 W for 5 minutes (5 seconds on and 5 seconds off) (Almasi et al., 2020; Mirzaee Moghaddam, & Rajaei, 2021).

#### 2.2.2. Particle size and zeta potential

The particle size distribution and zeta potential (ζ) of the dispersion of zein-BSG complexes, Pickering emulsion and nanoemulsion was determined using a Dynamic Light Scattering

(DLS) device (Anton Parr, Austria). Then, Span, $D_{10}$, $D_{50}$ and $D_{90}$ indices were obtained from the particle distribution curve (Javadi Farsani, Mirzaee Moghaddam, & Rajaei Najafabadi, 2023).

**2.2.3. Rheological properties**

The rheological properties of the dispersion of zein-BSG complexes, Pickering emulsion and nanoemulsion were evaluated using a rheometer (Modular Compact Rheometer, Antonparr, Austria) at a temperature of 25°C. The measurement of the flow behavior of samples was done with a concentric cylinder system. To investigate the flow behavior, the shear rate was linearly increased from 1 to 100 $s^{-1}$. To determine the viscoelastic properties of the samples, a strain sweep test was first performed to determine the linear viscoelastic range. Next, the frequency sweep test was performed in the linear viscoelastic range (1% strain) to measure the storage modulus (G') and the loss modulus (G") (Nazari, Rajaei, & Mirzaee Moghaddam, 2025).

**2.2.4. SEM**

Scanning electron microscope (SEM) was used to investigate the morphology of zein-BSG particles. First, the dispersion of particles was dried as a thin layer on a glass slide. Then, the surface of the sample was coated with gold by a desktop sputtering (DSR1, Nano Structure Coatings Company, Iran) and then the surface of the sample was imaged with a SEM (HV-300, Zeiss Sigma, Germany) (Mirzaee Moghaddam, 2019).

**2.3. Multilayer films containing REO emulsion**

**2.3.1. Preparation of multilayer films**

In this study, four types of films were prepared, all incorporating an emulsion in the central layer. The volumes of solution used for each layer were as follows: 10 mL for the first layer, 4 mL for the second layer, and 10 mL for the third layer. The film arrangements were as follows: Pectin-PE-Zein (pectin first layer + Pickering emulsion + zein third layer), Z-PE-P (pectin first layer + nanoemulsion + zein third layer), Zein-PE- Pectin (Zein first layer + Pickering emulsion + Pectin third layer), and Zein-NE- Pectin (Zein first layer + nanoemulsion + Pectin third layer). Each new layer was added only after the previous layer had dried (Cai, Xiao, Chen, & Liu, 2020; Nahalkar, Rajaei, & Mirzaee Moghaddam, in press a). Schematic of different stages of preparation of multilayer films is shown in Figure 1.

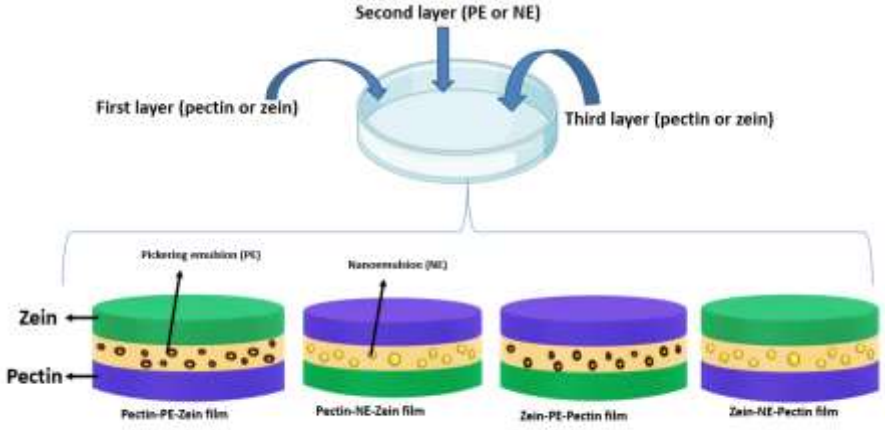


**Figure 1.** Schematic of different stages of preparation of multilayer films containing REO emulsion.

**2.3.2. Conditioning and film thickness**

Prior to testing, the film samples were conditioned for 48 hours in a chamber maintained at 50% relative humidity and 25°C. The thickness of the multilayer films was measured using a handheld micrometer (Mitotuyo No. 7327, Tokyo, Japan).

**2.3.3. Film structure**

To observe the microstructure of the films, various samples were cut into 10 × 10 mm pieces using a

razor blade. The surface and cross-sectional areas of these samples were coated with a 10 nm layer of gold. Subsequently, the samples were imaged using SEM (Du, Liu, Unsalan, Altunayar-Unsalan, Xiong, Manyande, & Chen, 2021; Nahalkar, Rajaei, & Mirzaee Moghaddam, in press b).

**2.3.4. Mechanical properties of films**

First, the films were cut into 5 × 2 cm specimens, and tensile tests were conducted using a universal testing machine (STM-20, Santam, Iran) at a speed of 10 mm/min. Tensile strength (TS, MPa) (Equation 1), elongation at break (EAB, %) (Equation 2), and Young's modulus (MPa) (Equation 3) were determined for each sample (Yan, Li, Wang, Lian, Fan, Xie, & Li, 2021).

$$\mathrm{TS} = \frac{\mathrm{Fm}}{\mathrm{T} \times \mathrm{W}} \quad (1)$$

$$\mathrm{EAB} = \frac{\mathrm{L_1 - L_0}}{\mathrm{L_0}} \times 100 \quad (2)$$

$$\mathrm{E} = \frac{stress}{\mathrm{strain}} \quad (3)$$

In Equation 1, Fm (N) represents the maximum force applied at the breaking point of the film, T (mm) denotes the film thickness, and W (mm) represents the film width. In Equation 2, L0 (mm) is the distance between the two jaws, and L1 (mm) is the length at the point of film rupture. Each test was performed in nine replicates.

**2.3.5. Physical properties of films**

**2.3.5.2. Moisture content, solubility and swelling index of films**

The moisture content (MC), solubility (WS), and swelling index (SI) of the films were determined after conditioning, using Equations (4), (5), and (6), respectively (Mohsenabadi, Rajaei, Tabatabaei, & Mohsenifar, 2018).

$$\mathrm{MC} = \frac{\mathrm{M_0 - M_1}}{\mathrm{M_0}} \times 100 \quad (4)$$

$$\mathrm{SI} = \frac{\mathrm{M_2 - M_1}}{\mathrm{M_1}} \times 100 \quad (5)$$

$$WS = \frac{\mathrm{M_1 - M_3}}{\mathrm{M_1}} \times 100 \quad (6)$$

In these equations, M0 represents the initial weight of the film, M1 is the weight of the film after drying in an oven at 105 °C, M2 is the weight of the swollen film, and M3 is the weight of the remaining film after 2 hours in water.

**2.3.5.3. Water vapor permeability**

The water vapor permeability (WVP) of the films was measured using a modified ASTM E96-05 standard method. Film samples were cut and affixed to the openings of glass vials (6 cm in height and 1 cm in opening diameter) containing 20 mL of distilled water. The vials were completely sealed with glue around the openings and placed in a desiccator containing silica gel (RH: 0%). Weight changes of the vials were recorded at specified intervals (Zhang, Huang, Shi, Liu, Zhang, & Zou, 2021).

$$\mathrm{WVP} = \frac{\Delta m \times X}{\Delta P \times S \times T} \quad (7)$$

Where $\Delta$m represents the change in weight (g), X is the average thickness (mm), $\Delta P$ is the pressure

difference on the two sides of the film (3169 Pa at 25℃), S is the cross-sectional area of the film ($m^2$), and T is the time interval (s).

**2.3.5.4. Color**

The color of the films was assessed using a colorimeter (Colorflex model A654-1005-60, USA). The parameters L* (lightness), a* (red/green), and b* (yellow/blue) were measured. Additionally, the overall color change (ΔE) was calculated using the equation provided by (Mirzaee Moghaddam, Khoshtaghaza, Barzegar, & Salimi, 2014; Barman, Das, & Badwaik, 2021).

Here, Δa, Δb, and ΔL represent the differences between the corresponding color values of the multilayer films and those of a standard white plate (a* = -0.10, b* = 3.32, L* = 93.11).

**2.3.5.6. X-ray Diffraction (XRD)**

The X-ray diffraction (XRD) patterns of the films were obtained using a Unisantis XMD 300 X-ray diffractometer (Unisantis Europe GmbH, Germany) at a temperature of 25 °C, over a 2θ range of 5-80° ( Shen, Ni, Thakur, Zhang, Hu, & Wei,, 2021; Mirzaee Moghaddam, Khoshtaghaza, Salimi, & Barzegar, 2014).

**2.3.6. Essential oil release from film and data analysis**

To investigate the release of REO, the films were cut into 2 × 2 cm pieces and attached to the plate of a glass vial (6 cm in height) containing 20 mL of pure ethanol. The vials were completely sealed. The amount of essential oil released into the ethanol was measured using a spectrophotometer (Unico, China) at a wavelength of 225 nm at intervals of 1, 2, 3, 4, 5, 6, 24, 48, 72, 96, and 120 hours, with measurements performed in triplicate. The essential oil release data were analyzed using DDsolver, a software package integrated into Excel. DDsolver employs various mathematical models to describe material release (Table 1). As shown in Table 1, each model has a different number of parameters. The best model was selected based on the correlation coefficient ($R^2$), Model Selection Criterion (MSC), and Akaike Information Criterion (AIC) (Kowalczyk, Kordowska-Wiater, Karaś, Zikeba, Mkeżyńska, & Wikacek, 2020).

**Table 1**. Models available in DDSolver for fitting REO release data.

| Model | Equation |
|---|---|
| **Zero-order** | $F = k_0 t$ |
| **First order** | $F = 100[1 - Exp(-k_1 t)]$ |
| **Higuchi** | $F = k_H t^{0.5}$ |
| **Hixson-Crowell** | $F = 100[1 - (k_{HC} t)^3]$ |
| **Hopfenberg** | $F = 100[1 - (1 - k_{HB} t)^n]$ |
| **Weibull** | $F = 100\{1 - Exp[-t^{\beta/\alpha}]\}$ |
| **Korsmeyer-Peppas** | $F = k_{KP} t^n$ |
| **Baker-Lonsdale** | $(3/2)\left[1 - (1 - F/100)^{2/3}\right] - \frac{F}{100} = k_{BL} t$ |
| **Makoid-Banakar** | $F = k_{MB} t^n Exp(kt)$ |
| **Logistic** | $F = 100\, Exp[(\alpha + \beta) log(t)]/\{1 + Exp[(\alpha + \beta) log(t)]\}$ |
| **Gompertz** | $F = 100\, Exp\{-\alpha Exp[-\beta log(t)]\}$ |
| **Probit** | $F = 100\Phi[(\alpha + \beta) log(t)]$ |

**2.4. Statistical analysis**

The data were processed using IBM SPSS version 22.0 for statistical evaluation. Mean values were compared through one-way analysis of variance (ANOVA) with Duncan's post hoc test, applying a 5% significance threshold. Graphical representations were created with SigmaPlot.

## 3. Results and discussion

### 3.1. Size and zeta potential of zein-BSG particles and REO emulsions

Figure 2a presents the distribution curve and ζ of the zein-BSG complex particles. The D50 of the zein-BSG particles was 306.9 nm, indicating that these complexes are formed within the nanometer range, below one micrometer. Smaller particles can provide better coverage of dispersed phase droplets and facilitate the formation of smaller emulsion droplets (Low, Siva, Ho, Chan, & Tey, 2020). Moreover, the ζ of the zein-BSG particles was measured at -15.1 mV, suggesting a higher density of negatively charged groups compared to positively charged groups on the particle surfaces. Given that BSG is an anionic gum, a negative ζ is expected (Abedini, Pircheraghi, Kaviani, & Hosseini, 2023). In addition, the distribution curves (Figure 2a) indicate that the droplet size of the Pickering emulsion (D50=1046.5 nm) was larger compared to that of the nanoemulsion (D50=90.1 nm). This result is likely due to the larger size of the zein-BSG complex particles used to stabilize the dispersed phase droplets compared to the smaller molecules of Tween 80. This finding is consistent with the study by Almasi et al. (2020), which demonstrated that the droplet size of a Pickering emulsion stabilized with whey-linolein protein isolate particles was greater than that of an emulsion stabilized with Tween 80. In addition, the ζ of Pickering emulsion droplets was approximately zero (-1.2 mV). This result indicates that the main mechanism in the stability of Pickering emulsion was steric. Figure 2b illustrates the morphology of the particle complex, showing that the particles are spherical. The morphology of particle complexes can influence their ability to form and stabilize Pickering emulsions, as the shape affects particle adsorption on the surface of dispersing phase droplets, potentially enhancing emulsion stability (Cui, Zhao, Guan, McClements, Liu, Liu, & Ngai, 2021).

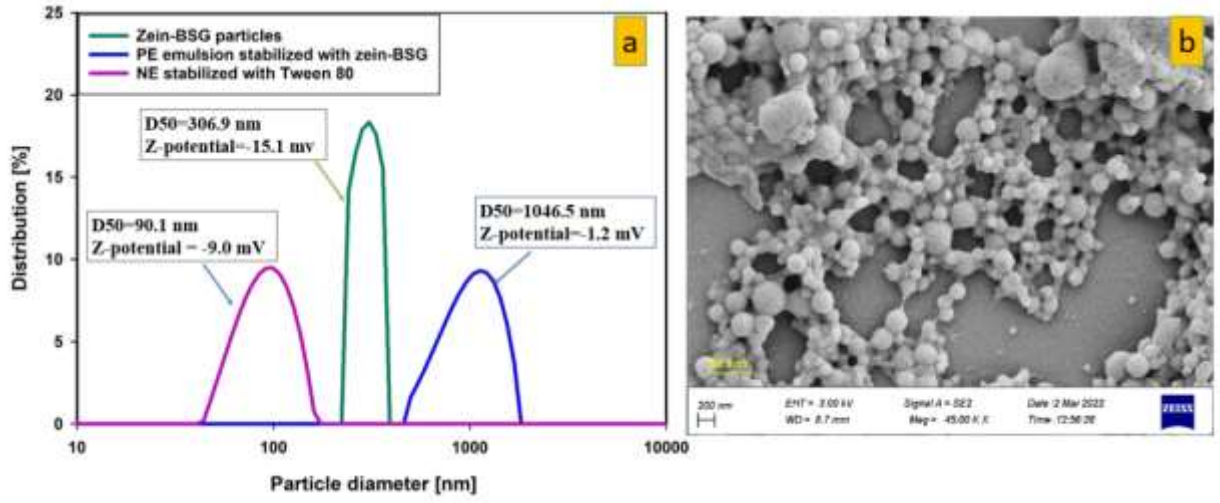


**Figure 2.** Particle size distribution of zein-BSG particle dispersion, REO Pickering emulsion and REO nanoemulsion (a), SEM images of zein-BSG particles (b).

### 3.2. Rheology of nanoemulsion and Pickering emulsion

Figure 3a presents the flow behavior of the zein-BSG particle dispersion, REO nanoemulsion (stabilized with Tween 80), and REO Pickering emulsion (stabilized with zein-BSG). According Figure 3a, the viscosity of the nanoemulsion was lower than that of the Pickering emulsion across different shear rates. The nanoemulsion exhibited nearly Newtonian flow behavior, corroborating the findings of others (Sanchez, Garc'ia, Mart'in-Piñero, Muñoz, & Alfaro-Rodr'iguez, 2022). In contrast, the Pickering emulsion displayed shear-thinning behavior, aligning with the observations of others (Li, Wu, Yin, Wu, Zhu, Gao, & Zhan, 2022). Notably, the flow behavior of the zein-BSG particle dispersion and the Pickering emulsion was approximately similar, suggesting that the flow behavior of the Pickering emulsion is influenced by the zein-BSG particles. Figures 3b and 3c depict the results of the strain and frequency sweeps for the zein-BSG particle dispersion and Pickering emulsion, respectively. The viscoelastic properties of the nanoemulsion were not investigated due to its nearly Newtonian flow behavior. The strain sweep test (Figure 2b) shows that the behavior of the zein-BSG dispersion and Pickering emulsion remained linear up to a strain of approximately 1%. The frequency sweep test (Figure 3c) indicates that at low frequencies, the G' was higher than the G" for both the zein-BSG dispersion and Pickering emulsion, signifying a gel-like structure. However, at high frequencies, the G" exceeded the G' for both samples, indicating that the gel-like structure was maintained by weak intermolecular forces (Zhao, Li, Wang, & Wang, 2023). It is also evident that the transition where G" surpasses G' occurred at a lower frequency for the Pickering emulsion compared to the zein-BSG particle dispersion. This result is likely due to the incorporation of non-polar REO molecules between the zein-BSG particles, which weakens the intermolecular forces among the particles.

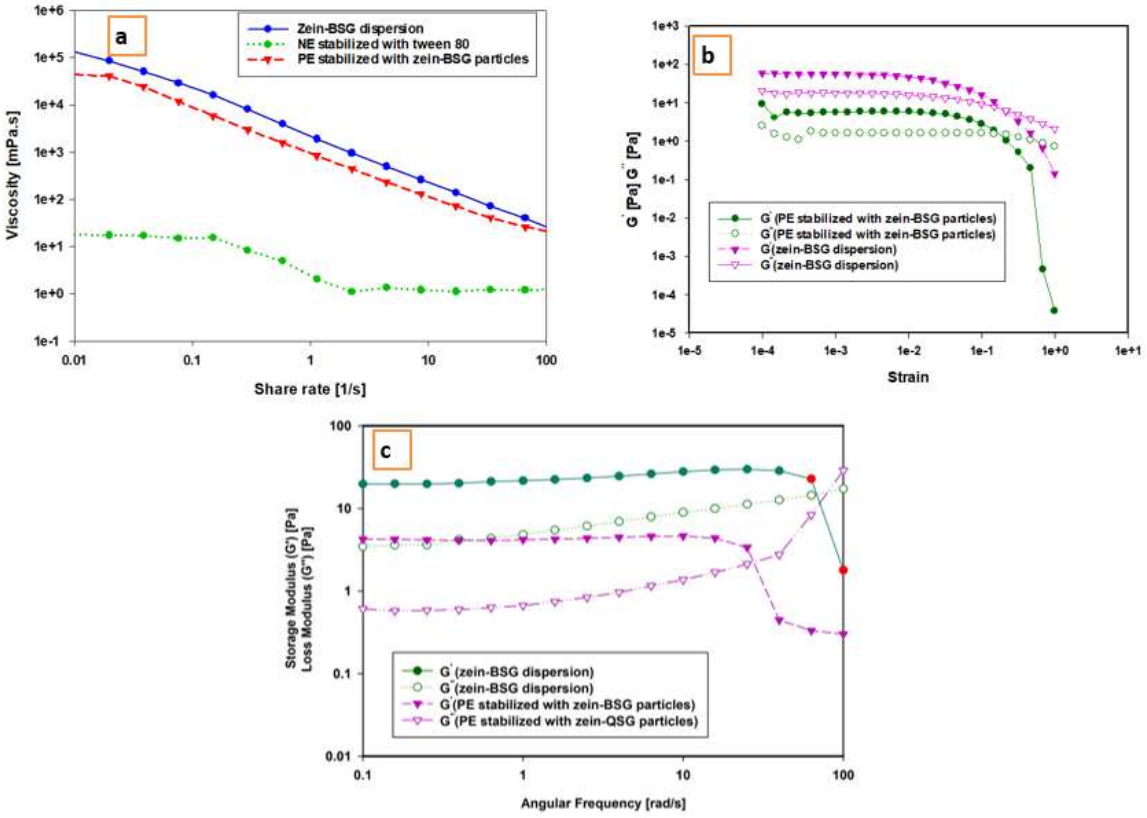


**Figure 3.** Flow behavior of zein-BSG dispersion, REO Pickering emulsion and REO nanoemulsion (a), strain sweep test (b) and frequency sweep test (c) of zein-BSG dispersion, and REO Pickering emulsion.

### 3.3. Characteristics of multilayer films

#### 3.3.1. Morphology of surface and cross-sectional of multilayer films

The microstructure of films is influenced by the interaction of constituent compounds and drying conditions, affecting various properties, including optical, resistance, and mechanical characteristics. Figure 4 presents SEM images of multilayer films from both surface and cross-sectional views. SEM images of surface show that films with a first pectin layer had a smoother surface compared to films with a first zein layer

.

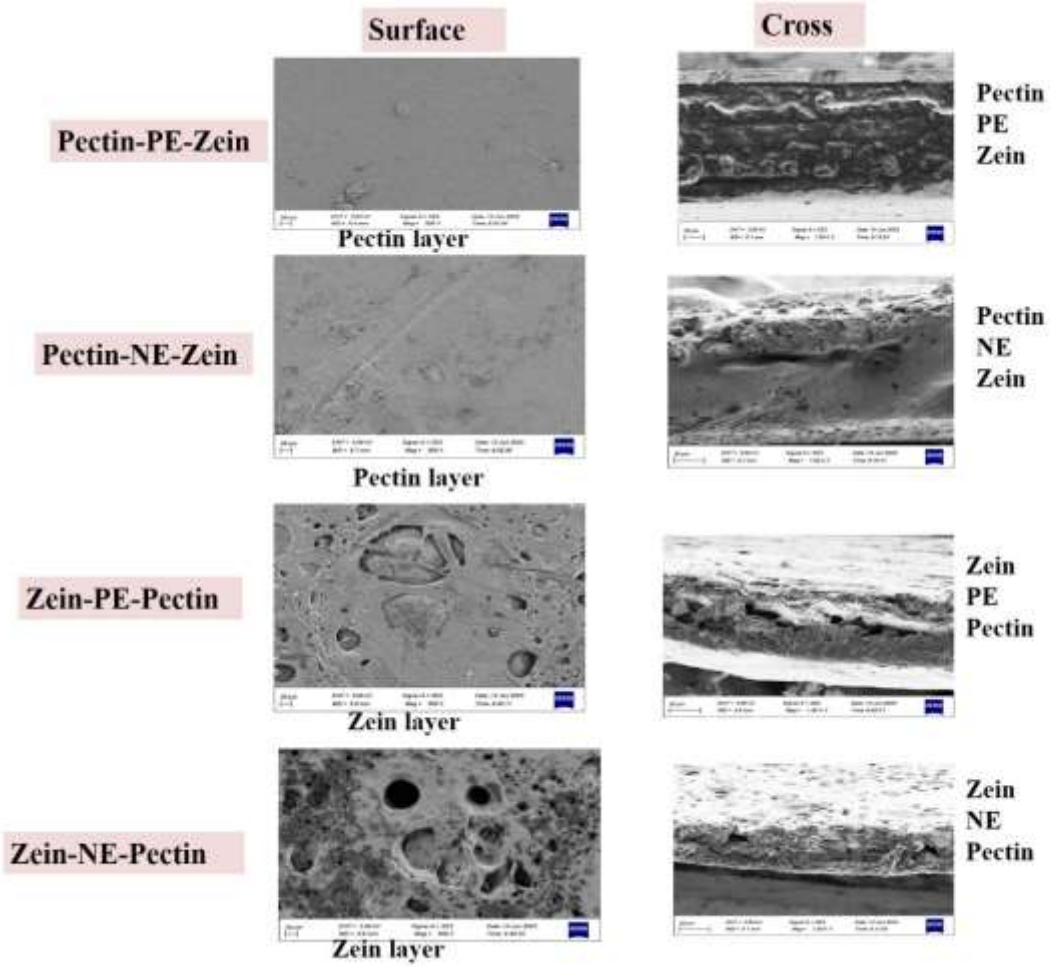


**Figure 4.** SEM images of the bottom surface and cross-section of various multilayer films.

The presence of more pores on the surface of the zein layer compared to the surface of the pectin layer could be related to the difference in polarity of pectin and zein. Pectin polymer is more polar compared to zein polymer. The greater polarity of pectin probably resulted in better interaction with the polar molecules of the plasticizer (glycerol) and consequently in greater homogeneity. The greater homogeneity of the pectin layer compared to the zein layer probably resulted in the formation of a smoother surface during the drying process. In the cross-sectional view (Figure 4), the bottom layer appeared denser than the top layer in all film samples. The upper layer contained more pores than the lower layer, likely due to the drying stage and the incorporation of the oily phase into the upper layer. As described in the methods section, the emulsion was added after drying the bottom layer, followed by the addition of the top layer. The lower viscosity of the oil phase compared to water likely resulted in greater penetration of the oil phase into the upper layer. This observation aligns with findings from previous studies, which indicated that adding an oil phase to the film alters its microstructure. Canhadas Bertan, Matta Fakhouri, Siani, & Ferreira Grosso, (2005) demonstrated that the inclusion of triacetin in gelatin film caused non-uniformity. Acosta, Jiménez, Cháfer, González-Mart'inez, & Chiralt, (2015) showed that incorporating a mixture of fatty

acid esters into the starch-gelatin film structure also resulted in non-uniformity.

### 3.3.2. Mechanical properties

The tensile strength (TS), elongation at break (EAB), and Young's modulus values of the multilayer films are presented in Figure 5. As shown in Figure 5a, film with pectin as the bottom layer and containing REO Pickering emulsion (PE) exhibited higher TS compared to other films.

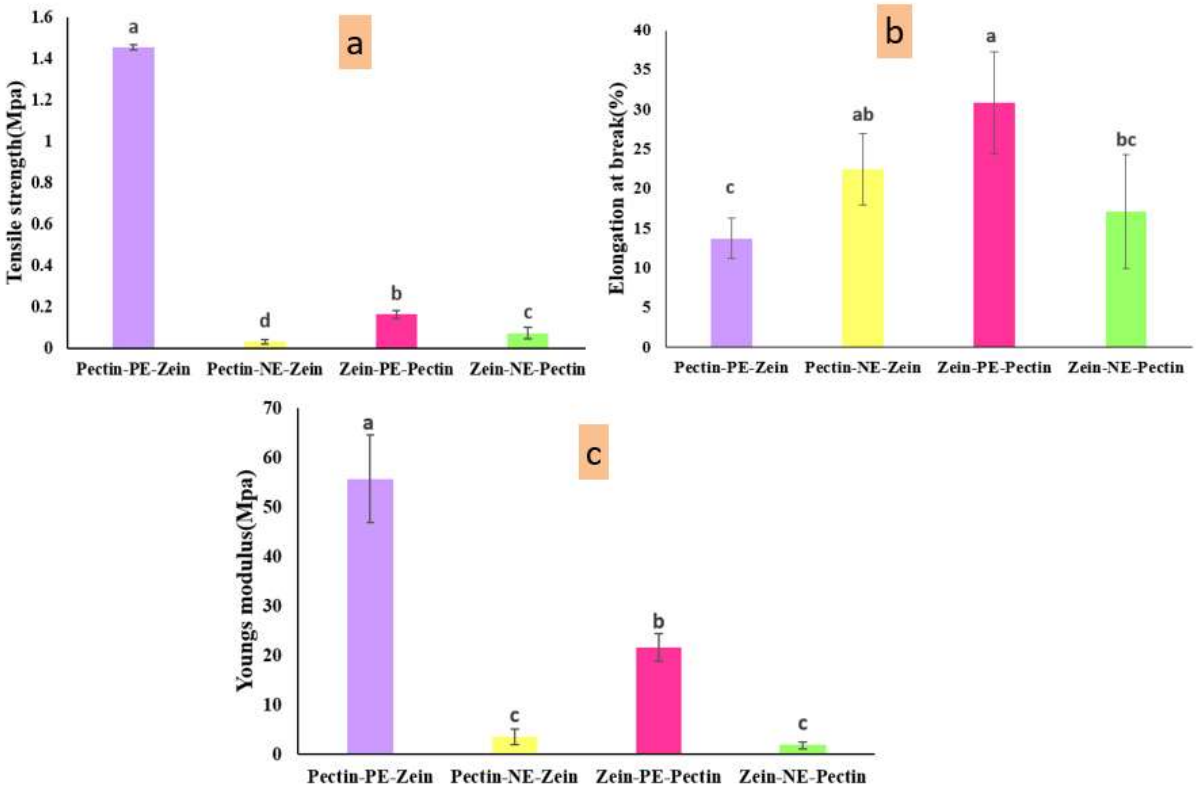


**Figure 5.** Tensile strength (a), elongation at break (b), and Young's modulus (c) of multilayer films.

This outcome is likely due to the more uniform structure of the pectin layer when used as the underlying layer, as evidenced by SEM images. Furthermore, a comparison between films containing nanoemulsion and those containing Pickering emulsion revealed that the TS was higher in films with Pickering emulsion, particularly in film with a pectin bottom layer. This increase in TS is probably attributable to the interaction of zein-BSG particles with the film-forming compounds, such as pectin and zein, which likely enhanced the structure and, consequently, the TS of films containing Pickering emulsions. These findings are consistent with the research of other scholars (Almasi et al., 2020; Zhu, Tang, Yin, & Yang, 2018). For instance, Zhu et al. (2018) suggested that the improved mechanical properties of polylactic acid-based films containing zein/chitosan particles may be related to the interaction at the interface between the polymer matrix and the Pickering emulsion stabilizing particles. Additionally, these results may be linked to the role of nanoemulsion as a plasticizer. Previous studies have demonstrated that nanoemulsions, acting as plasticizers, can interfere with the hydrogen bonding in films, thereby reducing stiffness and strength while increasing flexibility and mobility of

the polymer segments (Aghajani, Rafati, Aliahmadi, & Moghimi, 2024; da Silva, Reynaud, de Souza Picciani, e Silva, & Barradas, 2020). Figure 5b presents the EAB results for the different films. The data indicate that film with a zein underlayer had a higher EAB compared to those with a pectin underlayer, although no significant difference ($p > 0.05$) was observed among the treatments. In Figure 5c, the Young's modulus values of the multilayer films are shown. The trend in Young's modulus was similar to the TS results, suggesting that the same interpretations made for TS can be applied to the Young's modulus results.

### 3.3.3. Physical properties of multilayer films

#### 3.3.4.1. Water Vapor Permeability

The water vapor permeability (WVP) of the films is influenced by the hydrophilic-lipophilic balance of the film matrix (Acevedo-Fani, Salvia-Trujillo, Rojas-Graü, & Mart'in-Belloso, 2015). The WVP results for different films are shown in Figure 6a. Overall, the differences among the treatments were minimal. A significant difference ($p \leq 0.05$) was observed only between the Pectin-PE-Zein and other films, with the the Pectin-PE-Zein film exhibiting lower WVP. In general, it can be seen that films with a first pectin layer had lower permeability compared to films with a first zein layer. This result could be due to the higher porosity of the zein layer compared to the pectin layer, as SEM images also confirmed this finding. Also, according to Figure 6a, it can be seen that films containing Pickering emulsion had somewhat lower WVP compared to films containing nanoemulsion. The higher permeability of films containing nanoemulsion could be due to the presence of Tween 80 emulsifier. On the other hand, the zein-BSG particles probably interacted with other film components, including pectin and zein, to create a more cohesive structure. The results of this section showed that the use of Pickering emulsions can improve WVP compared to classical emulsions. Although the individual effects of the emulsion type and the layer type on WVP were minor, their combined effect resulted in a significant change in the WVP of the films.

#### 3.3.4.2. Moisture content, solubility and swelling index

The moisture content of various films is presented in Figure 6b. From this figure, it is evident that films with a zein bottom layer exhibited higher moisture content compared to those with a pectin bottom layer. This outcome is likely due to the more homogeneity and less porosity of the pectin layer relative to zein, resulting in less moisture escape when pectin was utilized as the top layer. Additionally, the type of emulsion had no significant effect on the moisture content of the films.

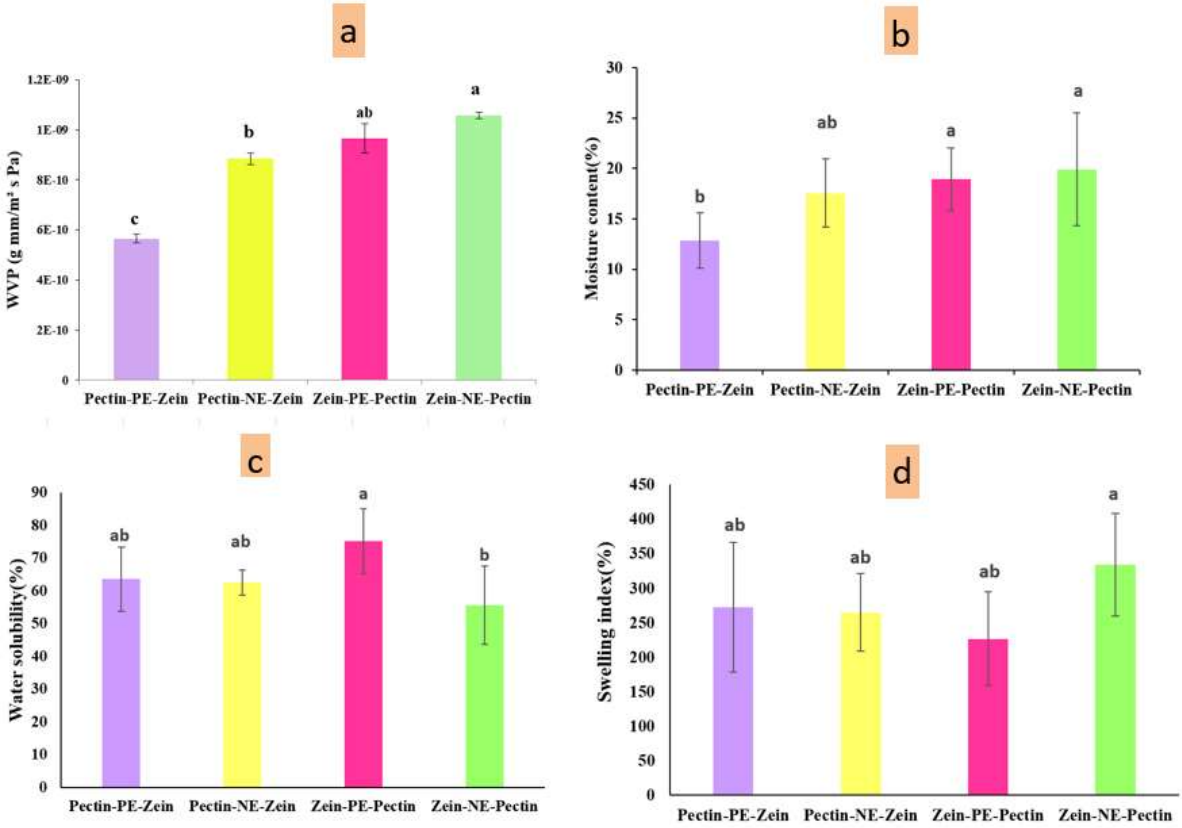


**Figure 6.** Water vapor permeability (a), moisture content (b), solubility (c), and swelling index (d) of multilayer films

Also, films containing Pickering emulsion had a lower moisture content compared to films containing nanoemulsion. This result could be due to the higher amount of essential oil in the structure of films containing Pickering emulsion compared to films containing nanoemulsion. Given the faster release of essential oil from nanoemulsion compared to Pickering emulsion, it is likely that there was a higher amount of essential oil in the structure of films containing Pickering emulsion. Aydogdu, Radke, Bezci, & Kirtil, (2020) explored the wettability of guar gum emulsion films containing orange essential oil, noting a decrease in moisture content with increased essential oil concentration. They explained that phenols in essential oils might bind to the hydroxyl groups of guar gum, thereby reducing the number of hydroxyl groups available for water interaction. The solubility results of different films are illustrated in Figure 6c. According to this figure, there were no significant differences ($p>0.05$) among the various treatments. This indicates that the layer arrangement and emulsion type did not significantly impact the solubility of the films. The swelling index results for the different films are shown in Figure 6d. The results of this figure show that neither the layer sequence nor the emulsion type significantly affected the swelling index.

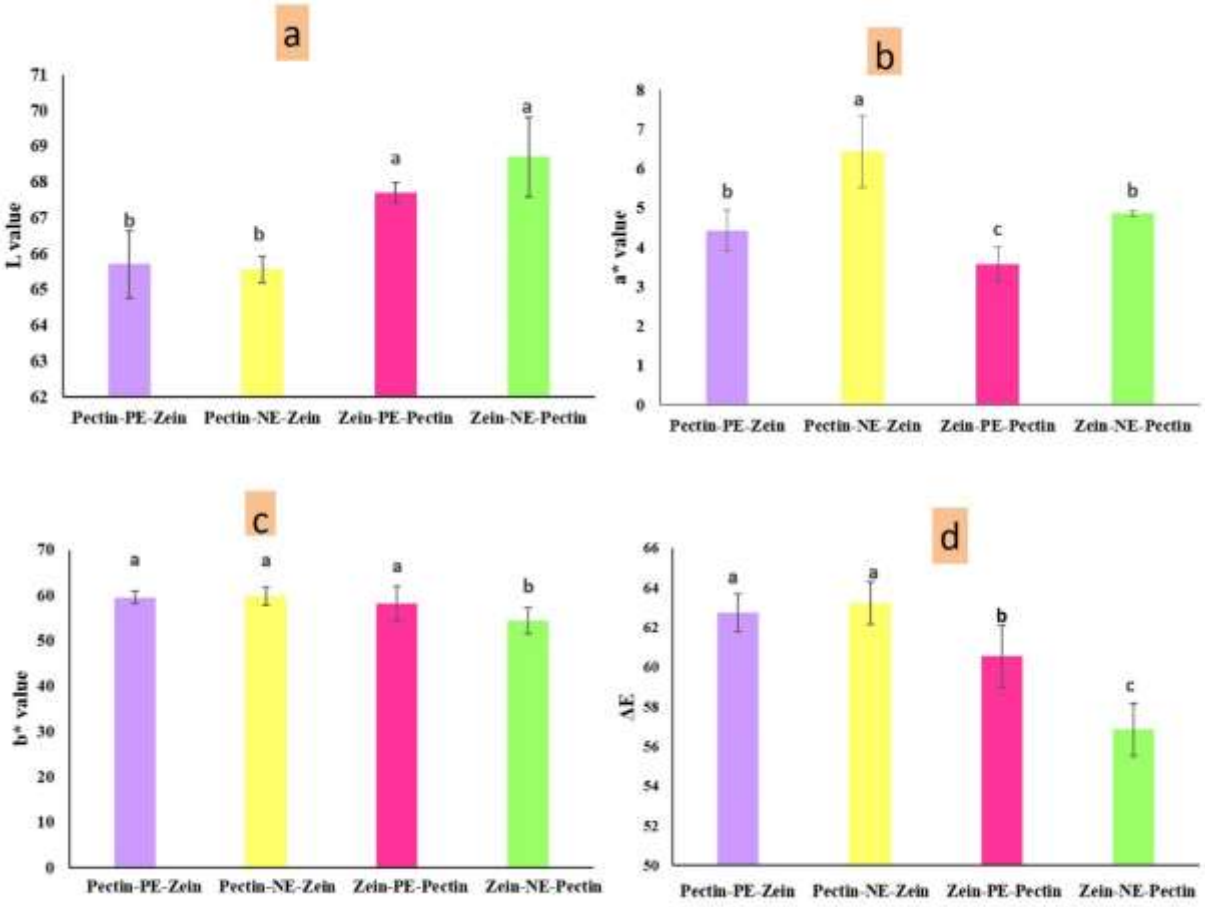


**Figure 7.** L* (a), a* (b), b* (c), ΔE (d), of multilayer films.

### 3.3.4.3. Color of films

Optical properties, including color and UV-Vis blocking ability, are critical attributes of food packaging films as they influence shelf life, visual appeal, and consumer purchasing decisions (Yadav, Behera, Chang, & Chiu, 2020). The color indices of different films are presented in Figure 7. The L* value, which indicates brightness, exceeded 65 for all films. According to Figure 7a, film with a zein underlayer containing NE exhibited the highest brightness index; however, no significant difference ($p>0.05$) was observed between treatments. The a* and b* values, representing green (negative)-red (positive) and blue (negative)-yellow (positive) color indices, respectively, were positive for all films (Figures 7b and 7c), indicating a tendency towards red and yellow hues. The type of emulsion and the order of layer hadn't significantly ($p>0.05$) effect on the a* and b* index. According to Figure 7d, the greatest ΔE was related to films with a pectin underlayer. Previous studies have shown that essential oils loaded in Pickering emulsions cause more color variation in pectin-based (Almasi et al., 2020) and soy polysaccharide-based films (Liu, Wang, Qi, Huang, & Xiao, 2019). Conversely, Ghadetaj, Almasi, & Mehryar, (2018) reported no significant change in the color properties of whey protein isolate films following the incorporation of nanoemulsion containing essential oil.

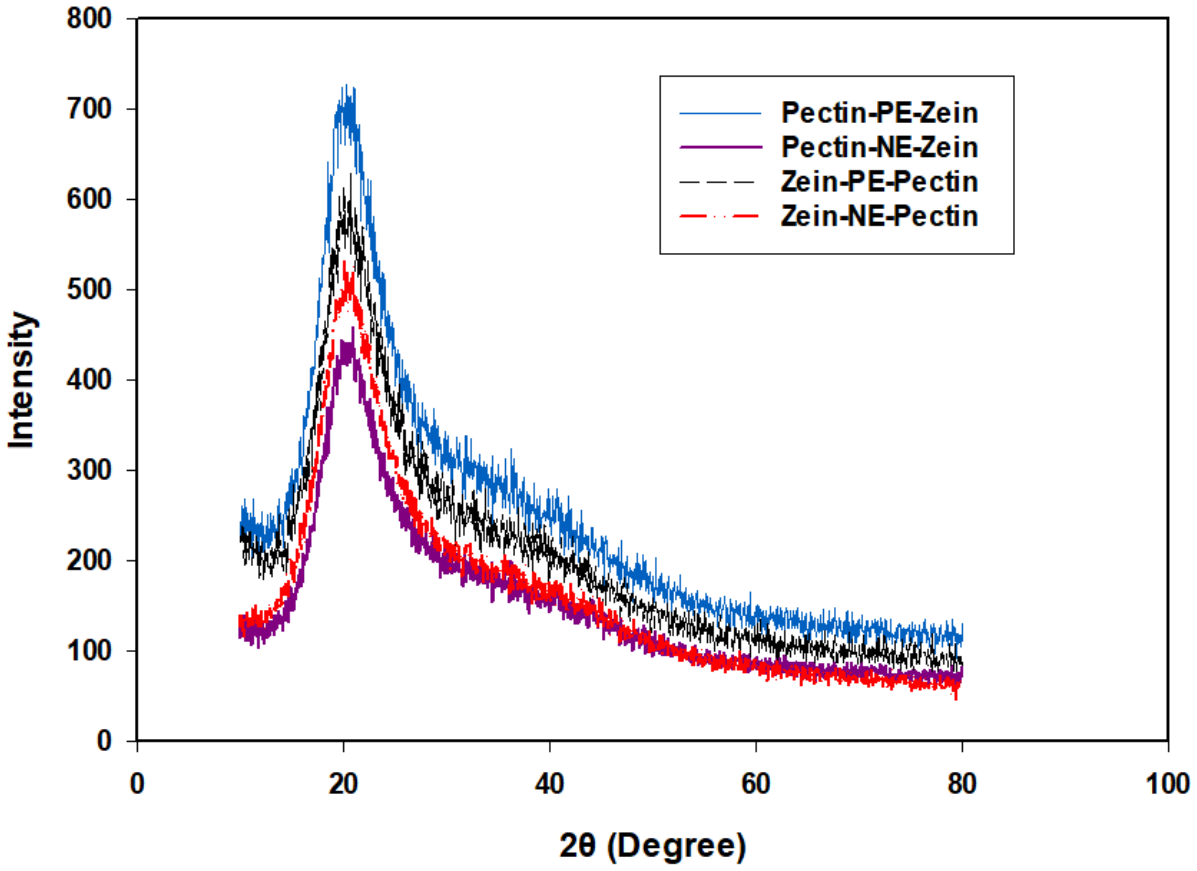


**Figure 8.** XRD spectra of multilayer films.

### 3.3.4.5. Crystallinity of films

The X-ray diffraction results of the films (Figure 8) revealed a broad peak at 2θ ≈ 20°, indicating the quasi-crystalline structure of pectin and the triple helix structure in zein (Ulrich, Lemos, Silva-Alvarez, Paiva, Gavioli, da Silva, & Francisco, 2023). Given the equal amounts of pectin and zein used in the films, the peak intensities were approximately similar across different films. This suggests that neither the emulsion type nor the layer addition order significantly affected the films' crystallinity. The separate layer addition of emulsions likely preserved the crystalline structure of the pectin and zein layers.

### 3.3.4.6. Essential oil release from multi-layer films

The cumulative release of essential oil from the films as a function of time is shown in Figure 9. Twelve mathematical models (Table 1) were employed to interpret the essential oil diffusion data from multilayer films. The best fit for each model was determined using $R^2$, AIC, and MSC indicators (Table 2). The Makoid-Banakar model demonstrated the highest $R^2$, lowest AIC, and highest MSC. The Makoid-Banakar models for different films are shown in Figure 9. According to literature, the Makoid-Banakar model describes release mechanisms involving skeletal dissolution and active substance release, aligning with theoretical predictions (Tang, Lu, Li, Shi, Zhang, Li, & Xu, 2022).

**Table 2:** Statistical parameters of different models to describe release of REO from different films

| Model | film | Statistical parameters | | |
|---|---|---|---|---|
| | | $R^2$ adjusted | AIC | MSC |
| Zero-order | Pectin-PE-Zein | -1.4321 | 56.3085 | -2.0761 |
| | Pectin-NE-Zein | -1.0608 | 61.7681 | -1.7654 |
| | Zein-PE-Pectin | -2.1247 | 56.6514 | -2.5781 |
| | Zein-NE-Pectin | -1.5176 | 61.5466 | -2.1196 |
| First order | Pectin-PE-Zein | -1.2961 | 55.8483 | -2.0186 |
| | Pectin-NE-Zein | -0.8024 | 60.6963 | -1.6315 |
| | Zein-PE-Pectin | -1.9897 | 56.2981 | -2.5339 |
| | Zein-NE-Pectin | -1.2777 | 60.7456 | -2.0195 |
| Higuchi | Pectin-PE-Zein | 0.0849 | 48.4884 | -1.0986 |
| | Pectin-NE-Zein | 0.3690 | 52.3000 | -0.5819 |
| | Zein-PE-Pectin | -0.3313 | 49.8262 | -1.7249 |
| | Zein-NE-Pectin | 0.1150 | 53.1824 | -1.0741 |
| Hixson-Crowell | Pectin-PE-Zein | -1.3429 | 56.0097 | -2.0387 |
| | Pectin-NE-Zein | -0.8929 | 61.0882 | -1.6804 |
| | Zein-PE-Pectin | -2.0363 | 56.4219 | -2.5494 |
| | Zein-NE-Pectin | -1.3620 | 61.0362 | -2.0558 |
| Hopfenberg | Pectin-PE-Zein | -1.6795 | 57.8504 | -2.2688 |
| | Pectin-NE-Zein | -1.1032 | 62.6978 | -1.8816 |
| | Zein-PE-Pectin | -2.4886 | 58.2996 | -2.7841 |
| | Zein-NE-Pectin | -1.6579 | 62.7473 | -2.2697 |
| Weibull | Pectin-PE-Zein | 0.9226 | 29.4929 | 1.2759 |
| | Pectin-NE-Zein | 0.9980 | 6.9978 | 5.0808 |
| | Zein-PE-Pectin | 0.9167 | 28.4221 | 0.9506 |
| | Zein-NE-Pectin | 0.9844 | 21.6576 | 2.8665 |
| Korsmeyer-Peppas | Pectin-PE-Zein | 0.9245 | 29.3005 | 1.2999 |
| | Pectin-NE-Zein | 0.9980 | 6.9553 | 5.0862 |
| | Zein-PE-Pectin | 0.9174 | 28.3531 | 0.9592 |
| | Zein-NE-Pectin | 0.9839 | 21.8911 | 2.8374 |
| Baker-Lonsdale | Pectin-PE-Zein | 0.1596 | 47.8072 | -1.0134 |
| | Pectin-NE-Zein | 0.4808 | 50.7403 | -0.3870 |
| | Zein-PE-Pectin | -0.2441 | 49.2841 | -1.6571 |
| | Zein-NE-Pectin | 0.2366 | 52.0004 | -0.9263 |
| Makoid-Banakar | **Pectin-PE-Zein** | **0.9847** | **21.7561** | **2.2430** |
| | **Pectin-NE-Zein** | **0.9989** | **7.5881** | **5.0071** |
| | **Zein-PE-Pectin** | **0.9685** | **25.8727** | **1.2693** |
| | **Zein-NE-Pectin** | **0.9955** | **16.9151** | **3.4594** |
| Logistic | Pectin-PE-Zein | 0.9209 | 29.6675 | 1.2540 |
| | Pectin-NE-Zein | 0.9978 | 7.7913 | 4.9817 |
| | Zein-PE-Pectin | 0.9160 | 28.4854 | 0.9427 |
| | Zein-NE-Pectin | 0.9848 | 21.4488 | 2.8926 |
| Gompertz | Pectin-PE-Zein | 0.9152 | 30.2272 | 1.1841 |
| | Pectin-NE-Zein | 0.9965 | 11.4414 | 4.5254 |
| | Zein-PE-Pectin | 0.9138 | 28.6980 | 0.9161 |

| | | | | |
|---|---|---|---|---|
| | Zein-NE-Pectin | 0.9859 | 20.8255 | 2.9706 |
| Probit | Pectin-PE-Zein | 0.9185 | 29.9037 | 1.2245 |
| | Pectin-NE-Zein | 0.9975 | 8.6801 | 4.8706 |
| | Zein-PE-Pectin | 0.9151 | 28.5764 | 0.9313 |
| | Zein-NE-Pectin | 0.9853 | 21.1754 | 2.9268 |

The Makoid-Banakar model's k values for different multilayer films ranged from 0 to 0.007, indicating a close similarity to the Korsmeyer-Peppas model, which is commonly used to describe slow release kinetics. The parameter n in the Korsmeyer-Peppas model, which characterizes release mechanisms, ranged from 0.037 to 0.24 for different films, indicating pseudo-Fickian diffusion (Abdul Rasool, Mohammed, & Salem, 2021; Tang et al., 2022). This suggests a weak interaction between essential oil compounds and film-forming substances, justified by the hydrophobic nature of essential oils and the hydrophilic nature of most film-forming compounds. Films with a pectin underlayer exhibited greater essential oil release compared to those with a zein underlayer. The more hydrophobic structure of zein likely caused stronger interactions with essential oils, resulting in reduced release. Furthermore, films with NE released essential oil more rapidly than those with PE. The thicker layer around the oily phase in Pickering emulsions resulted in a more gradual release compared to nanoemulsions. These findings align with other studies, indicating that the layer addition order and emulsion type affect essential oil release (Almasi et al., 2020; Ghadetaj et al., 2018). Zhu et al. (2018) noted that encapsulating thymol essential oil in Pickering emulsion resulted in slower release of the essential oil from the film structure. Almasi et al. (2020) showed that essential oil release was higher in films containing nanoemulsion compared to those with Pickering emulsion. Most studies on films containing essential oils focus on single-layer films, where similar release occurs from both sides (Zhang, Zhang, Huang, Shi, Muhammad, Zhai, & Zou, 2023; Zhang, Pu, Jiang, Chen, Shen, Zhang, & Jiang, 2024), causing a significant portion of essential oils to enter the environment rather than affecting the food. Based on these results, using pectin as the inner layer and zein as the outer layer of packaging could enhance essential oil release into the package interior. Thus, well-designed multilayer edible films can optimize essential oil release at the food-contact side. Furthermore, suitable encapsulation methods can achieve optimal essential oil release, with nanoemulsions and Pickering emulsions being effective for rapid and gradual release, respectively.

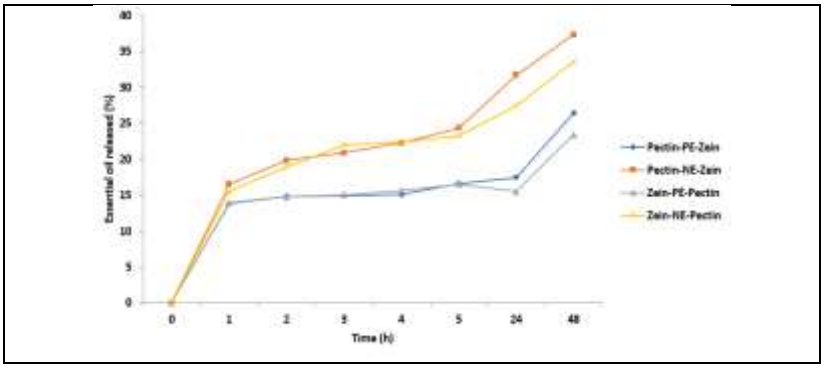

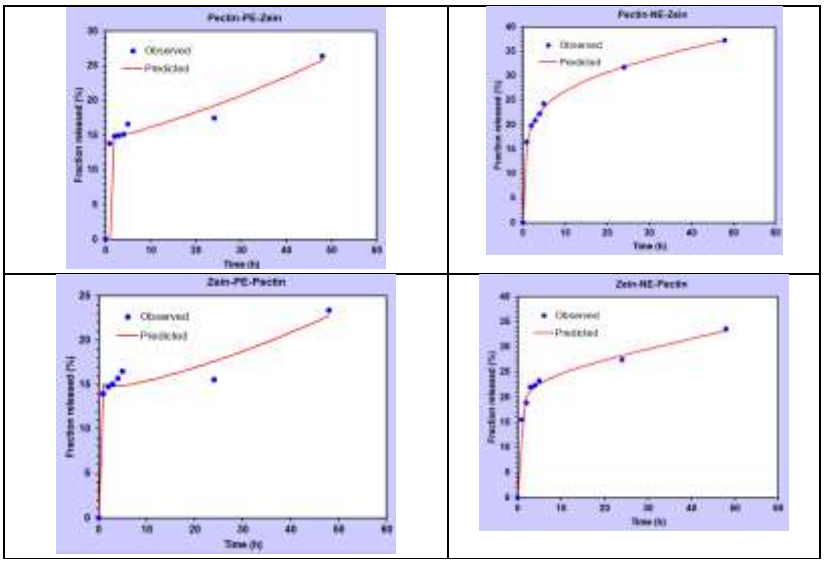


**Figure 9.** Cumulative release profiles of REO from multilayer films and the Makoid-Banakar models for different films; experimental (●) and theoretical data (lines).

## 4. Conclusion

This study demonstrated that the layer sequence and encapsulation method significantly influence the physicochemical properties and release behavior of zein-pectin multilayer films containing REO. The zein-BSG complex particles effectively stabilized Pickering emulsions, which exhibited shear-thinning behavior and gel-like viscoelastic properties, contrasting with the near-Newtonian flow of Tween 80-stabilized nanoemulsions. Multilayer films with pectin as the bottom layer displayed smoother surfaces, higher tensile strength, and lower water vapor permeability compared to zein-based films, attributed to pectin's superior structural homogeneity. Pickering emulsions enhanced mechanical properties due to particle-matrix interactions, while nanoemulsions acted as plasticizers, increasing flexibility. Essential oil release followed pseudo-Fickian diffusion, with pectin-bottomed films and nanoemulsions facilitating faster release, whereas zein layers and Pickering emulsions prolonged retention. The Makoid-Banakar model best described the release kinetics, highlighting the potential for tailored EO delivery in active packaging. These findings suggest that strategic layer arrangement—using pectin as the inner layer and zein as the outer layer—can improve REO release toward the food interface, minimizing environmental loss. Furthermore, encapsulation method selection (nanoemulsion for rapid release, Pickering emulsion for sustained release) allows customization based on application needs. This study provides valuable insights for designing functional biodegradable films with controlled antimicrobial and antioxidant properties for food preservation. In future research, scale-up studies should address industrial production challenges, particularly regarding the consistency of Pickering emulsion formation at larger volumes. Additionally, the development of hybrid encapsulation systems combining Pickering and nanoemulsion technologies may enable precise temporal control of antimicrobial delivery.

## References

[1] Alias, A. R., Wan, M. K., & Sarbon, N. M. (2022). Emerging materials and technologies of multi-layer film for food packaging application: A review. *Food Control*, *136*, 108875.

[2] Gupta, V., Biswas, D., & Roy, S. (2022). A

comprehensive review of biodegradable polymer-based films and coatings and their food packaging applications. *Materials*, *15*(17), 5899.

[3] Yang, Y., Du, Y., Gupta, V. K., Ahmad, F., Amiri, H., Pan, J., & Rajaei, A. (2024). Exploring blockchain and artificial intelligence in intelligent packaging to combat food fraud: A comprehensive review. *Food Packaging and Shelf Life*, *43*, 101287.

[4] Mutlu-Ingok, A., Devecioglu, D., Dikmetas, D. N., Karbancioglu-Guler, F., & Capanoglu, E. (2020). Antibacterial, antifungal, antimycotoxigenic, and antioxidant activities of essential oils: An updated review. Molecules, 25(20), 4711.

[5] Akhter, R., Masoodi, F. A., & Wani, T. A. (2024). Chitosan, gelatin and pectin based bionanocomposite films with rosemary essential oil as an active ingredient for future foods. *International Journal of Biological Macromolecules*, 132813.

[6] Shahrampour, D., & Razavi, S. M. A. (2023). Fabrication and characterization of novel biodegradable active films based on Eremurus luteus root gum incorporated with nanoemulsions of rosemary essential oil. *Progress in Organic Coatings*, *175*, 107360.

[7] Zhang, X., Ismail, B. B., Cheng, H., Jin, T. Z., Qian, M., Arabi, S. A., & Guo, M. (2021). Emerging chitosan-essential oil films and coatings for food preservation-A review of advances and applications. *Carbohydrate Polymers*, *273*, 118616.

[8] Zhang, W., Jiang, H., Rhim, J.-W., Cao, J., & Jiang, W. (2022). Effective strategies of sustained release and retention enhancement of essential oils in active food packaging films/coatings. *Food Chemistry*, *367*, 130671.

[9] Hosseini, E., Rajaei, A., Tabatabaei, M., Mohsenifar, A., & Jahanbin, K. (2019). Preparation of Pickering Flaxseed Oil-in-Water Emulsion Stabilized by Chitosan-Myristic Acid Nanogels and Investigation of Its Oxidative Stability in Presence of Clove Essential Oil as Antioxidant. Food Biophysics, 1–13.

[10] Sharkawy, A., Barreiro, M. F., & Rodrigues, A. E. (2020). Chitosan-based Pickering emulsions and their applications: A review. *Carbohydrate Polymers*, 116885.

[11] Pandita, G., de Souza, C. K., Gonçalves, M. J., Jasińska, J. M., Jamróz, E., & Roy, S. (2024). Recent progress on Pickering emulsion stabilized essential oil added biopolymer-based film for food packaging applications: A review. *International Journal of Biological Macromolecules*, 132067.

[12] Sharkawy, A., & Rodrigues, A. E. (2024). Plant gums in Pickering emulsions: A review of sources, properties, applications, and future perspectives. *Carbohydrate Polymers*, 121900.

[13] Yang, Y., Gupta, V. K., Du, Y., Aghbashlo, M., Show, P. L., Pan, J., & Rajaei, A. (2023). Potential application of polysaccharide mucilages as a substitute for emulsifiers: A review. *International Journal of Biological Macromolecules*, 124800.

[14] Chen, H., Wang, Q., Rao, Z., Lei, X., Zhao, J., Lei, L., & Ming, J. (2023). The linear/nonlinear rheological behaviors of Pickering emulsion stabilized by Zein and Xanthan gum: Effect of interfacial assembly strategies. *Food Hydrocolloids*, *145*, 109116.

[15] Wu, B., Zhang, S., Jiang, X., Hou, P., Xin, Y., Zhang, L., & Zhou, D. (2022). Impact of weakly charged insoluble karaya gum on zein nanoparticle and mechanism for stabilizing Pickering emulsions. *International Journal of Biological Macromolecules*, *222*, 121–131.

[16] Almasi, H., Azizi, S., & Amjadi, S. (2020). Development and characterization of pectin films activated by nanoemulsion and Pickering emulsion stabilized marjoram (Origanum majorana L.) essential oil. *Food Hydrocolloids*, *99*, 105338.

[17] Alinaqi, Z., Khezri, A., & Rezaeinia, H. (2021). Sustained release modeling of clove essential oil from the structure of starch-based bio-nanocomposite film reinforced by electrosprayed zein nanoparticles. *International Journal of Biological Macromolecules*, *173*, 193–202.

[18] Papadaki, A., Lappa, I. K., Manikas, A. C., Carbone, M. G. P., Natsia, A., Kachrimanidou, V., & Kopsahelis, N. (2024). Grafting bacterial cellulose nanowhiskers into whey protein/essential oil film composites: Effect on structure, essential oil release and antibacterial properties of films. *Food Hydrocolloids*, *147*, 109374.

[19] Jouki, M., Yazdi, F. T., Mortazavi, S. A., & Koocheki, A. (2013). Physical, barrier and antioxidant properties of a novel plasticized edible film from quince seed mucilage. *International Journal of Biological Macromolecules*, *62*, 500–507.

[20] Mirzaee Moghaddam, H., & Rajaei., A. (2021). Effect of Pomegranate Seed Oil Encapsulated in Chitosan-capric Acid Nanogels Incorporating Thyme Essential Oil on Physicomechanical and Structural Properties of Jelly Candy. Journal of Agricultural Machinery, 11(2), 37-49. doi:10.22067/jam.v4i1.33163

[21] Javadi Farsani, M., Mirzaee Moghaddam, H., & Rajaei Najafabadi, A. (2023). Study of some qualitative and organoleptic properties of enriched apple leather. Journal of food science and technology (Iran), 19(133), 175-186.

[22] Nazari, N., Rajaei, A., & Mirzaee Moghaddam, H. (2025). Comparative Effects of Basil Seed and Cress Seed Gums on Stability of Flaxseed Oil Pickering Emulsion and Functional Kiwifruit Bar Characteristics. Food Biophysics, 20(2), 1–15.

[23] Mirzaee Moghaddam, H. (2019). Investigation of PhysicoMechanical Properties of Functional Gummy Candy Fortified with Encapsulated Fish Oil in Chitosan-Stearic Acid Nanogel by Pickering Emulsion Method. Journal of food science and technology (Iran). 16 (90) 53-64. https://doi.org/10.1111/j.1365-2621.1989.tb05978.x

[24] Cai, J., Xiao, J., Chen, X., & Liu, H. (2020). Essential oil loaded edible films prepared by continuous casting method: Effects of casting cycle and loading position on the release properties. *Food Packaging and Shelf Life*, *26*, 100555.

[25] Nahalkar, A. Rajaei, A., & Mirzaee Moghaddam, H. (in press a). Investigation of the possibility of producing a stabilized walnut oil emulsion with chia seed mucilage and its application in edible films. Journal of Food Science and Technology (FSCT). Article ID: 78673.

[26] Du, H., Liu, C., Unsalan, O., Altunayar-Unsalan, C., Xiong, S., Manyande, A., & Chen, H. (2021). Development and characterization of fish myofibrillar protein/chitosan/rosemary extract composite edible films and the improvement of lipid oxidation stability during the grass carp fillets storage. *International Journal of Biological Macromolecules*, *184*, 463–475. https://doi.org/10.1016/j.ijbiomac.2021.06.121

[27] Nahalkar, A. Rajaei, A., & Mirzaee Moghaddam, H. (in press b). Investigation of some structural and physicomechanical properties of bilayer and composite edible films based on sodium carboxymethyl cellulose. Journal of Agricultural Machinery. Doi: 10.22067/jam.2025.90690.1312.

[28] Yan, J., Li, M., Wang, H., Lian, X., Fan, Y., Xie, Z., & Li, W. (2021). Preparation and property studies of chitosan-PVA biodegradable antibacterial multilayer films doped with Cu2O and nano-chitosan composites. *Food Control*, *126*, 108049.

[29] Mohsenabadi, N., Rajaei, A., Tabatabaei, M., & Mohsenifar, A. (2018). Physical and antimicrobial properties of starch-carboxy methyl cellulose film containing rosemary essential oils encapsulated in chitosan nanogel. International Journal of Biological Macromolecules, 112, 148–155.

[30] Zhang, J., Huang, X., Shi, J., Liu, L., Zhang, X., & Zou, X. (2021). A visual bi-layer indicator based on roselle anthocyanins with high hydrophobic property for monitoring griskin freshness. *Food Chemistry*, *355*, 129573.

[31] Mirzaee Moghaddam, H., Khoshtaghaza, M. H., Barzegar, M., & Salimi, A. (2014). effect of potassium permanganate nano-zeolite and storage time on physicochemical properties of kiwifruit (Hayward). Journal of Agricultural Machinery. 4(1): 37-49.

[32] Barman, M., Das, A. B., & Badwaik, L. S. (2021). Effect of xanthan gum, guar gum, and pectin on physicochemical, color, textural, sensory, and drying characteristics of kiwi fruit leather. *Journal of Food Processing and Preservation*, *45*(5), e15478.

[33] Shen, Y., Ni, Z.-J., Thakur, K., Zhang, J.-G., Hu, F., & Wei, Z.-J. (2021). Preparation and characterization of clove essential oil loaded nanoemulsion and pickering emulsion activated pullulan-gelatin based edible film. *International Journal of Biological Macromolecules*, *181*, 528–539.

[34] Mirzaee Moghaddam, H., Khoshtaghaza, M. H., Salimi, A., & Barzegar, M. (2014). The TiO2–Clay-LDPE nanocomposite packaging films: investigation on the structure and physicomechanical properties. Polymer-Plastics Technology and Engineering, 53(17), 1759-1767.

[35] Kowalczyk, D., Kordowska-Wiater, M., Karaś, M., Zikeba, E., Mkeżyńska, M., & Wikacek, A. E. (2020). Release kinetics and antimicrobial properties of the potassium sorbate-loaded edible films made from pullulan, gelatin and their blends. *Food Hydrocolloids*, *101*, 105539.

[36] Low, L. E., Siva, S. P., Ho, Y. K., Chan, E. S., & Tey, B. T. (2020). Recent advances of characterization techniques for the formation, physical properties and stability of Pickering emulsion. Advances in Colloid and Interface Science, 277, 102117. https://doi.org/10.1016/j.cis.2020.102117

[37] Abedini, A. A., Pircheraghi, G., Kaviani, A., & Hosseini, S. (2023). Exploration of curcumin-incorporated dual anionic alginate-quince seed gum films for transdermal drug delivery. *International Journal of Biological Macromolecules*, *248*, 125798.

[38] Cui, F., Zhao, S., Guan, X., McClements, D. J., Liu, X., Liu, F., & Ngai, T. (2021). Polysaccharide-based Pickering emulsions: Formation, stabilization and applications. *Food Hydrocolloids*, *119*, 106812.

[39] Sanchez, A., Garc'ia, M. C., Mart'in-Piñero, M. J., Muñoz, J., & Alfaro-Rodr'iguez, M.-C. (2022). Elaboration and characterization of nanoemulsion with orange essential oil and pectin. *Journal of the Science of Food and Agriculture*, *102*(9), 3543–3550.

[40] Li, H., Wu, C., Yin, Z., Wu, J., Zhu, L., Gao, M., & Zhan, X. (2022). Emulsifying properties and bioavailability of clove essential oil Pickering emulsions stabilized by octadecylaminated carboxymethyl curdlan. *International Journal of Biological Macromolecules*, *216*, 629–642.

[41] Zhao, X., Li, D., Wang, L., & Wang, Y. (2023). Role of gelation temperature in rheological behavior and microstructure of high elastic starch-based emulsion-filled gel. *Food Hydrocolloids*, *135*, 108208.

[42] Canhadas Bertan, L., Matta Fakhouri, F., Siani, A. C., & Ferreira Grosso, C. R. (2005). Influence of the addition of lauric acid to films made from gelatin, triacetin and a blend of stearic and palmitic acids. In *Macromolecular symposia* (Vol. 229, pp. 143–149).

[43] Acosta, S., Jiménez, A., Cháfer, M., González-Mart'inez, C., & Chiralt, A. (2015). Physical properties and stability of starch-gelatin based films as affected by the addition of esters of fatty acids. *Food Hydrocolloids*, *49*, 135–143.

[44] Zhu, J.-Y., Tang, C.-H., Yin, S.-W., & Yang, X.-Q. (2018). Development and characterization of novel antimicrobial bilayer films based on Polylactic acid (PLA)/Pickering emulsions. *Carbohydrate Polymers*, *181*, 727–735.

[45] Aghajani, F., Rafati, H., Aliahmadi, A., & Moghimi, R. (2024). Novel Nanoemulsion-Loaded Hydroxyl propyl methyl cellulose Films as Bioactive Food Packaging Materials Containing Satureja khuzestanica Essential Oil. *Carbohydrate Polymer Technologies and Applications*, 100544.

[46] da Silva, T. N., Reynaud, F., de Souza Picciani, P. H., e Silva, K. G. de H., & Barradas, T. N. (2020). Chitosan-based

films containing nanoemulsions of methyl salicylate: Formulation development, physical-chemical and in vitro drug release characterization. *International Journal of Biological Macromolecules*, *164*, 2558–2568.

[47] Acevedo-Fani, A., Salvia-Trujillo, L., Rojas-Graü, M. A., & Mart'in-Belloso, O. (2015). Edible films from essential-oil-loaded nanoemulsions: Physicochemical characterization and antimicrobial properties. *Food Hydrocolloids*, *47*, 168–177.

[48] Aydogdu, A., Radke, C. J., Bezci, S., & Kirtil, E. (2020). Characterization of curcumin incorporated guar gum/orange oil antimicrobial emulsion films. *International Journal of Biological Macromolecules*, *148*, 110–120. https://doi.org/10.1016/j.ijbiomac.2019.12.255

[49] Yadav, M., Behera, K., Chang, Y.-H., & Chiu, F.-C. (2020). Cellulose nanocrystal reinforced chitosan based UV barrier composite films for sustainable packaging. *Polymers*, *12*(1), 202.

[50] Liu, Q.-R., Wang, W., Qi, J., Huang, Q., & Xiao, J. (2019). Oregano essential oil loaded soybean polysaccharide films: Effect of Pickering type immobilization on physical and antimicrobial properties. *Food Hydrocolloids*, *87*, 165–172.

[51] Ghadetaj, A., Almasi, H., & Mehryar, L. (2018). Development and characterization of whey protein isolate active films containing nanoemulsions of Grammosciadium ptrocarpum Bioss. essential oil. *Food Packaging and Shelf Life*, *16*, 31–40.

[52] Ulrich, G. D., Lemos, A. G., Silva-Alvarez, A. C. F., Paiva, L. B., Gavioli, R. R., da Silva, L. L., & Francisco, K. R. (2023). Zein/hydroxypropylcellulose biofilms with hydrophilic and hydrophobic montmorillonite clays. *Polymer Composites*, *44*(5), 2634–2644.

[53] Tang, Y., Lu, Y., Li, L., Shi, C., Zhang, X., Li, X., & Xu, W. (2022). Electrostatic Induced Peptide Hydrogels for pH-Controllable Doxorubicin Release and Antitumor Activity. *ChemistrySelect*, *7*(36), e202202284.

[54] Abdul Rasool, B. K., Mohammed, A. A., & Salem, Y. Y. (2021). The optimization of a dimenhydrinate transdermal patch formulation based on the quantitative analysis of in vitro release data by DDSolver through skin penetration studies. *Scientia Pharmaceutica*, *89*(3), 33.

[55] Zhang, J., Zhang, J., Huang, X., Shi, J., Muhammad, A., Zhai, X., & Zou, X. (2023). Study on cinnamon essential oil release performance based on pH-triggered dynamic mechanism of active packaging for meat preservation. *Food Chemistry*, *400*, 134030.

[56] Zhang, Y., Pu, Y., Jiang, H., Chen, L., Shen, C., Zhang, W., & Jiang, W. (2024). Improved sustained-release properties of ginger essential oil in a Pickering emulsion system incorporated in sodium alginate film and delayed postharvest senescence of mango fruits. *Food Chemistry*, *435*, 137534.

**مجله علوم و صنایع غذایی ایران**

سایت مجله: www.fsct.modares.ac.ir

**مقاله علمی_پژوهشی**

# مدل‌سازی رهایش اسانس رزماری از فیلم‌های چندلایه زئین-پکتین:تأثیر توالی لایه‌ها و روش درونپوشانی بر خواص فیلم

**احمد رجایی[1*]، نرگس نظری[2]، حسین میرزایی مقدم[3*]**

۱- دانشیار، تکنولوژی موادغذایی، دانشکده کشاورزی، دانشگاه صنعتی شاهرود.

۲- کارشناسی ارشد علوم و مهندسی صنایع غذایی، دانشکده کشاورزی، دانشگاه صنعتی شاهرود.

۳- استادیار، مکانیک بیوسیستم، دانشکده کشاورزی، دانشگاه صنعتی شاهرود.

**اطلاعات مقاله**

**تاریخ های مقاله :**

**تاریخ دریافت: ۱۴۰۴/۰۲/۲۷**

**تاریخ پذیرش: ۱۴۰۴/۰۴/۱۰**

**کلمات کلیدی:**

بسته‌بندی فعال،

فیلم‌های زیست‌تخریب‌پذیر،

نانوامولسیون،

امولسیون پیکرینگ.

**DOI: 10.48311/fsct.2025.84050.0**

* مسئول مکاتبات:

ahmadrajaei@gmail.com

Hosseinsg@yahoo.com

**چکیده**

فیلم‌های فعال زیست‌تخریب‌پذیر حاوی اسانس‌ها اغلب با چالش‌هایی نظیر نگهداری ضعیف اسانس و خواص فیزیکومکانیکی نامطلوب مواجه هستند. در این مطالعه، تأثیر ترتیب لایه‌ها و روش کپسوله‌سازی (نانوامولسیون در مقایسه با امولسیون پیکرینگ) بر سینتیک رهایش و خواص فیزیکومکانیکی فیلم‌های چندلایه زئین-پکتین حاوی اسانس رزماری مورد بررسی قرار گرفت. نانوذرات کمپلکس زئین-صمغ دانه ریحان (با قطر متوسط D50 nm 306.9 =و پتانسیل زتا ζ= -15.1 mV) به‌منظور پایدارسازی امولسیون‌های پیکرینگ (D50=1046,50 nm) سنتز شدند، در حالی که نانوامولسیون‌های (D50=90,10 nm) پایدارشده با توئین ۸۰ عنوان نمونه کنترل استفاده شدند. تحلیل رئولوژیکی نشان داد که امولسیون‌های پیکرینگ رفتار برشی-رقیق از خود نشان دادند، در حالی که نانوامولسیون‌ها دارای جریان تقریباً نیوتنی بودند. فیلم‌های چندلایه‌ای که پکتین در لایه زیرین آن‌ها به‌کار رفته بود، در مقایسه با فیلم‌های با لایه زیرین زئین، دارای سطحی صاف‌تر، استحکام کششی بالاتر و نفوذپذیری نسبت به بخار آب کمتری بودند که به همگنی بالاتر پکتین نسبت داده شد. افزودن امولسیون پیکرینگ موجب افزایش استحکام کششی و کاهش نفوذپذیری، به‌دلیل تعامل ذرات با ماتریس شد. در حالی که نانوامولسیون‌ها به‌عنوان نرم‌کننده عمل کرده و انعطاف‌پذیری را افزایش دادند. رهایش اسانس رزماری از مدل انتشار شبه-فیکی تبعیت کرد. فیلم‌های دارای لایه زیرین پکتین و نانوامولسیون‌ها، رهایش سریع‌تری را نشان دادند. در حالی که لایه‌های زئین و امولسیون‌های پیکرینگ باعث افزایش پایداری و نگهداری اسانس شدند. نتایج این پژوهش نشان داد که با تنظیم راهبردی ترتیب لایه‌ها و انتخاب نوع امولسیون می‌توان رهایش اسانس و عملکرد فیلم‌های فعال را بهبود بخشید و راه‌حل‌هایی هدفمند برای بسته‌بندی فعال مواد غذایی ارائه داد.